Method for quantifiying conduction velocity during ventricular fibrillation

Ayman Mourad* and Martyn P. Nash†
Bioengineering Institute, The University of Auckland, New Zealand
(Received 7 June 2006; revised manuscript received 31 August 2006; published 17 January 2007)

Velocity of propagation of electrical excitation in the heart is important for the understanding of complex arrhythmias such as ventricular fibrillation (VF). In this paper, we present a method to estimate the conduction velocity of electrical activation wavefronts that are defined to be a particular isovalue of any scalar field, such as electrical activation times, electrical phase, or indeed any other quantity that can be used to determine excitation wavefronts. This general method is based on tracking trajectories of material points that are assumed to be embedded within the wavefronts, whilst the direction of propagation is assumed to be perpendicular to the wavefront. We have derived an explicit expression for the conduction velocity in terms of the spatiotemporal gradients of the scalar field used to define wavefronts. Moreover, although it is often difficult to use activation times to compute conduction velocities during complex VF, we show that other scalar fields such as detrended voltage or electrical phase, which can faithfully represent the electrical activity during fibrillatory conduction, can be used to determine conduction velocities. We demonstrate the application of our method to determine conduction velocities from contact mapping recordings over the entire epicardial surface of the fibrillating pig heart.

DOI: 10.1103/PhysRevE.75.011914 PACS number(s): 87.10.+e, 94.30.Tz, 87.19.Nn, 87.19.Hh

I. INTRODUCTION

Mechanisms underpinning ventricular fibrillation (VF) remain incompletely understood, although the existence of dominant re-entrant sources (mother rotors), and multiple wavelets have both been implicated [1]. Vulnerabilities to the onset and maintenance of VF have been linked to dynamic properties of wavefront propagation [2], such as the spatiotemporal evolution of conduction velocity distributions during regional cardiac ischemia, and the dependence of wave speed on activation frequency (i.e., conduction velocity restitution).

Quantification of conduction velocity during VF remains challenging. Conventional methods have classically relied on the ability to determine activation times at electrodes [3–5]. It is clear that simply dividing the distance between two electrodes by the difference in their activation times can yield spurious estimates of conduction velocity if the direction of wavefront propagation is not aligned with the segment connecting these electrodes [6]. On the other hand, if the electrode alignment is in the direction of wavefront propagation, then the above method provides a realistic estimate of the conduction velocity. Thus, the calculation of conduction velocity requires the determination of wavefront propagation direction, however, it can be difficult to determine these wavefront directions from activation times, particularly during complex VF [7]. To address the problem of determining wavefront direction, previously published methods have computed conduction velocity using spatial gradients of the activation time field [6–8]. However, determining the activation time field during complex fibrillatory activity is inherently ambiguous [7].

A recent study presents a method for estimating conduction velocity that is based on fitting splines to isopotential contours of voltage [9]. Their method adopts the conventional approach of dividing the distance swept out by a wavefront (or waveback) across a number of frames by the time taken to propagate this distance. They demonstrate that this method is applicable to wavefronts with a variety of shapes. However, their method was not applied to complex activation patterns such as multiple-wavelet VF in this report.

In order to determine conduction velocity during complex VF, we have developed a general method that does not implicitly require the determination of an activation time field, nor the use of wavefronts in successive frames. Instead, our method computes conduction velocity using the spatiotemporal gradients of any scalar field for which a particular isovalue delineates excitation wavefronts. The method effectively tracks material particles that are assumed to be embedded within wavefronts, and assumes that the direction of propagation is perpendicular to the wavefront. Here we present the theoretical development of our method, together with illustrations of its application for the analysis of conduction velocity on the surface of the pig heart during organized and complex VF.

II. CONDUCTION VELOCITY

A. Activation wavefronts and trajectories

We treat the propagation of electrical excitation through myocardial tissue as a wave-like phenomenon, and begin by considering the motion of a material particle P embedded within the wavefront. We denote the position of P at time instant t as $\mathbf{x}_P(t)$. The trajectory of the particle, $\mathcal{T}_P$, is the set of successive locations occupied by P:

$$\mathcal{T}_P = \{\mathbf{x}_P(t); t \geqslant 0\}. \quad (1)$$

*a.mourad@auckland.ac.nz
†martyn.nash@auckland.ac.nz

The Lagrangian description of the velocity of P at time instant t is

$$\mathbf{V}_{\mathrm{P}}(t) = \frac{d\mathbf{x}_{\mathrm{P}}(t)}{dt}. \tag{2}$$

We now examine the behavior at a fixed spatial point M with location $\mathbf{x}=(x,y,z)$. We assume that the particle P is located at position M at time instant t, and that at some later time $t+\Delta t$, a different particle Q occupies the location M:

$$\mathbf{x}_{\mathrm{P}}(t) = \mathbf{x}_{\mathrm{Q}}(t+\Delta t). \tag{3}$$

Let $\mathbf{v}(\mathbf{x},t)$ denote the velocity of the particle located at M at time instant t. Using an Eulerian frame of reference, the trajectory of the particle P is given by

$$\mathcal{T}_{\mathrm{P}} = \left\{ \mathbf{x} \text{ such that } \frac{d\mathbf{x}}{dt} = \mathbf{v}(\mathbf{x},t) \right\}. \tag{4}$$

The Lagrangian and Eulerian descriptions of $\mathbf{V}_{\mathrm{P}}(t)$ and $\mathbf{v}(\mathbf{x},t)$ are related using

$$\mathbf{V}_{\mathrm{P}}(t) = \mathbf{v}(\mathbf{x}_{\mathrm{P}}(t),t). \tag{5}$$

Now consider the case of the propagation of electrical excitation through cardiac tissue. We define the activation wavefronts as the isolines [in two dimensions (2D)] or the isosurfaces (in 3D) of a given scalar field, such as activation time or electrical phase. Let $F_{\mathrm{P}}(t)$ and $f(\mathbf{x},t)$ be the Lagrangian and the Eulerian representations, respectively, of the selected scalar field. Thus

$$F_{\mathrm{P}}(t) = f(\mathbf{x}_{\mathrm{P}}(t),t). \tag{6}$$

Without loss of generality, we assume that the wavefront at time instant t, WF(t), is defined to be the isoline (or the isosurface) of zero (in general, any given isovalue would suffice here):

$$\mathrm{WF}(t) = \{\mathbf{x} \text{ such that } f(\mathbf{x},t) = 0\}. \tag{7}$$

Let P be a material particle embedded within the wavefront WF(0) at time instant zero. Thus $F_{\mathrm{P}}(0)=0$. We then track the particle during wavefront propagation. Therefore, along the trajectory $\mathcal{T}_{\mathrm{P}}$ we have

$$F_{\mathrm{P}}(t) = 0 \quad \forall\, t \geqslant 0. \tag{8}$$

Consequently, the time rate of change of $F_{\mathrm{P}}(t)$ is also zero, thus

$$\frac{\partial F_{\mathrm{P}}(t)}{\partial t} = \frac{Df(\mathbf{x}_{\mathrm{P}},t)}{Dt} = \frac{\partial f(\mathbf{x}_{\mathrm{P}},t)}{\partial t} + \mathbf{v}(\mathbf{x}_{\mathrm{P}},t)\cdot\nabla f(\mathbf{x}_{\mathrm{P}},t) = 0, \tag{9}$$

where Df/Dt denotes the particle derivative and ∇f denotes the spatial gradient of f.

B. Closed form expressions for conduction velocity

In order to determine an explicit expression for the conduction velocity, Eq. (9) must be combined with constraints on the wavefronts. To this end, we assume that the conduction velocity $\mathbf{v}(\mathbf{x},t)$ is perpendicular to the wavefront, which is consistent with previous studies [3,5–7,9,10].

1. Excitation in a 2D plane or 3D volume

For electrical activity in a 2D plane or 3D volume, since the conduction velocity $\mathbf{v}(\mathbf{x},t)$ is assumed to be perpendicular to the wavefront, then $\mathbf{v}(\mathbf{x},t)$ is parallel to the normal of the wavefront $\mathbf{N}(\mathbf{x},t)$. Using this, the conduction velocity can be obtained by solving Equation (9) to yield

$$\mathbf{v}(\mathbf{x},t) = \frac{-1}{\lambda(\mathbf{x},t)}\frac{\partial f(\mathbf{x},t)}{\partial t}\mathbf{N}(\mathbf{x},t),$$

where

$$\lambda(\mathbf{x},t) = \mathbf{N}(\mathbf{x},t)\cdot\nabla f(\mathbf{x},t). \tag{10}$$

Since wavefronts correspond to $f(\mathbf{x},t)=0$, then the normal vector $\mathbf{N}(\mathbf{x},t)$ can be defined using

$$\mathbf{N}(\mathbf{x},t) = \nabla f(\mathbf{x},t). \tag{11}$$

Substituting this into Eq. (10), yields the general form of the conduction velocity for activity in a 2D plane or a 3D volume:

$$\mathbf{v}(\mathbf{x},t) = \frac{-\nabla f(\mathbf{x},t)}{|\nabla f(\mathbf{x},t)|^2}\frac{\partial f(\mathbf{x},t)}{\partial t}. \tag{12}$$

Note that if the spatial gradient of the field is zero (i.e., if the field is constant) over a particular region, then the wavefront normal cannot be defined, and consequently, the conduction velocity cannot be defined across this region.

For the special case in which wavefronts are defined as the isochrones of the activation time $T(\mathbf{x})$, the scalar field f can be defined as $f(\mathbf{x},t)=T(\mathbf{x})-t$. Consequently, a simplified relationship for the conduction velocity based on activation times is given by

$$\mathbf{v}(\mathbf{x}) = \frac{\nabla T(\mathbf{x})}{|\nabla T(\mathbf{x})|^2} \tag{13}$$

which has been previously published [6,7].

When dealing with a surface in 3D space, $\nabla f(\mathbf{x},t)$ is not necessarily tangent to the surface. However, the vector normal to the wavefront lies on the surface, thus Eq. (11) does not apply. One way to address this issue is to use a 2D parametrization of the surface in 3D space, as explained in the next section.

2. Excitation on a surface

For the analysis of propagation of electrical excitation on an infinitesimally thin surface, activation wavefronts correspond to 1D curves located on the surface. In this case, the conduction velocity vector is perpendicular to the wavefront and tangent to the surface. We define the surface using the parameters (u,v):

$$\mathbf{S}(u,v) = (S_x(u,v),S_y(u,v),S_z(u,v)). \tag{14}$$

The trajectory of a particle P embedded within a wavefront in the surface is then given by

$$x(t) = S_x(u(t),v(t)); \quad y(t) = S_y(u(t),v(t));$$

$$z(t) = S_z(u(t),v(t)), \tag{15}$$

and the conduction velocity $\mathbf{v}=(v_x,v_y,v_z)$ is given by

$$\mathbf{v} = \frac{\partial \mathbf{S}}{\partial u}\dot{u} + \frac{\partial \mathbf{S}}{\partial v}\dot{v}, \tag{16}$$

which ensures that $\mathbf{v}$ is tangent to the surface.

If f is the scalar field defined over the surface and is now considered to be a function of (u,v,t), then we have

$$F_P(t) = f(u(t),v(t),t) = 0, \tag{17}$$

and the particle derivative of f is

$$\frac{\partial F_P(t)}{\partial t} = \frac{Df(u,v,t)}{Dt} = \frac{\partial f(u,v,t)}{\partial t} + \frac{\partial f}{\partial u}\dot{u} + \frac{\partial f}{\partial v}\dot{v} = 0. \tag{18}$$

The assumption that the conduction velocity is perpendicular to the wavefront requires that

$$\mathbf{v} \cdot \boldsymbol{\tau} = 0, \tag{19}$$

where $\boldsymbol{\tau}$ denotes a vector that is tangent to the wavefront, and is given by (see the Appendix)

$$\boldsymbol{\tau} = \frac{\partial \mathbf{S}}{\partial u}\frac{\partial f}{\partial v} - \frac{\partial \mathbf{S}}{\partial v}\frac{\partial f}{\partial u}. \tag{20}$$

The quantities $\dot{u}$ and $\dot{v}$ are obtained by solving Eqs. (18) and (19), and are given by

$$\dot{u} = \frac{1}{\lambda}\left[\left(\frac{\partial \mathbf{S}}{\partial u}\cdot\frac{\partial \mathbf{S}}{\partial v}\right)\frac{\partial f}{\partial v} - \left|\frac{\partial \mathbf{S}}{\partial v}\right|^2\frac{\partial f}{\partial u}\right]\frac{\partial f}{\partial t},$$

$$\dot{v} = \frac{1}{\lambda}\left[\left(\frac{\partial \mathbf{S}}{\partial u}\cdot\frac{\partial \mathbf{S}}{\partial v}\right)\frac{\partial f}{\partial u} - \left|\frac{\partial \mathbf{S}}{\partial u}\right|^2\frac{\partial f}{\partial v}\right]\frac{\partial f}{\partial t}, \tag{21}$$

where

$$\lambda = \left|\frac{\partial \mathbf{S}}{\partial u}\right|^2\left(\frac{\partial f}{\partial v}\right)^2 - 2\left(\frac{\partial \mathbf{S}}{\partial u}\cdot\frac{\partial \mathbf{S}}{\partial v}\right)\frac{\partial f}{\partial u}\frac{\partial f}{\partial v} + \left|\frac{\partial \mathbf{S}}{\partial v}\right|^2\left(\frac{\partial f}{\partial u}\right)^2.$$

Substituting $\dot{u}$ and $\dot{v}$ into Eq. (16) yields a closed form expression for the conduction velocity on the surface.

In the case where

$$\left|\frac{\partial \mathbf{S}}{\partial u}\right| = \left|\frac{\partial \mathbf{S}}{\partial v}\right| = 1 \quad \text{and} \quad \frac{\partial \mathbf{S}}{\partial u}\cdot\frac{\partial \mathbf{S}}{\partial v} = 0, \tag{22}$$

Eq. (21) simplifies to

$$\dot{u} = \frac{-1}{\lambda}\frac{\partial f}{\partial u}\frac{\partial f}{\partial t}, \quad \dot{v} = \frac{-1}{\lambda}\frac{\partial f}{\partial v}\frac{\partial f}{\partial t}, \quad \text{where } \lambda = \left(\frac{\partial f}{\partial u}\right)^2 + \left(\frac{\partial f}{\partial v}\right)^2. \tag{23}$$

This simplified form has been previously used to estimate conduction velocity on the ventricular epicardial surface using the activation time field, where a local Cartesian fiber coordinate system was defined at each point on the surface [8]. However, their coordinate system does not satisfy Eq. (22) and thus neglects the effects of surface curvature on the conduction velocity estimate.

In the clinical setting, cardiac electrograms are typically recorded at the endocardium or epicardium using balloon catheters or contact electrode arrays. It is important to note that in this case, the recording surface is an external boundary of an excitable 3D volume (the myocardium). Therefore, a recorded wavefront corresponds to the intersection of a 3D isosurface of excitation propagation with the external boundary. Consequently, the conduction velocity that we compute on the surface using Eq. (12) or Eqs. (16) and (21) does not represent the true conduction velocity of the 3D intramural wavefront. Instead, we are examining the *apparent* conduction velocity of the wavefront at the surface of the tissue.

3. Uniqueness of the conduction velocity

We now show that the calculation of the conduction velocity is equivalent regardless of the field that is chosen to define activation wavefronts. To this end, consider $f(\mathbf{x},t)$ and $g(\mathbf{x},t)$ to be two arbitrary scalar fields with particular isovalues that delineate activation wavefronts. If $\mathbf{v}_f(\mathbf{x},t)$ and $\mathbf{v}_g(\mathbf{x},t)$ denote the conduction velocities obtained from f and g, respectively, then it can be shown that $\mathbf{v}_f(\mathbf{x},t)=\mathbf{v}_g(\mathbf{x},t)$, $\forall \mathbf{x},t$.

We provide the proof for the particular case when we can define the activation time field. Let $T(\mathbf{x})$ denote the activation time field, and let $f(\mathbf{x},t)$ denote any other scalar field with zero isovalues that correspond to the activation wavefronts. Consequently, the following equation is implicitly satisfied:

$$\forall \mathbf{x}, \quad f(\mathbf{x},T(\mathbf{x})) = 0, \tag{24}$$

thus the spatial gradient is identically zero:

$$\forall \mathbf{x}, \quad \nabla f(\mathbf{x},T(\mathbf{x})) + \frac{\partial f}{\partial t}(\mathbf{x},T(\mathbf{x}))\nabla T(\mathbf{x}) = 0. \tag{25}$$

If we substitute Eqs. (24) and (25) into the general expression for the conduction velocity [Eq. (12)], we get

$$\mathbf{v}_f(\mathbf{x},T(\mathbf{x})) = \frac{-\nabla f(\mathbf{x},T(\mathbf{x}))}{|\nabla f(\mathbf{x},T(\mathbf{x}))|^2}\frac{\partial f}{\partial t}(\mathbf{x},T(\mathbf{x})) = \frac{\nabla T(\mathbf{x})}{|\nabla T(\mathbf{x})|^2}, \tag{26}$$

resulting in the same expression for the conduction velocity as given in Eq. (13), which is calculated directly from the activation time field. Thus we have demonstrated the theoretical equivalence of the conduction velocity as computed from T and any other field f (such as electrical phase) whose zero isovalues correspond to the activation wavefronts. In the next section, we present a numerical comparison of these relations using experimental recordings from the fibrillating pig heart.

III. APPLICATION TO EXPERIMENTAL DATA

A. Methods

1. Data acquisition

As previously described [11], a 29 kg pig was anesthetized, artificially ventilated, thoracotomized, and instru-

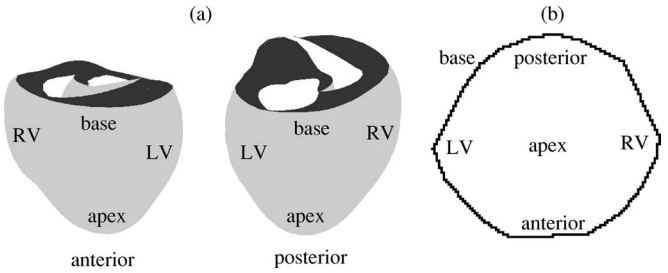

FIG. 1. (a) 3D representation of the ventricles. (b) 2D polar projection showing anatomical orientation.

mented with an elasticized sock containing 280 unipolar contact electrodes (inter-electrode spacing 5–10 mm) connected to a UnEmap system (Auckland UniServices Limited, New Zealand) with the reference electrode attached to the chest retractors. During an episode of spontaneous VF, 10 s of electrical activity was sampled at 1 kHz over the entire ventricular epicardium.

Subsequently, the electrode sock was placed over a heart-shaped model of similar dimension to the pig heart, and the 3D locations of the epicardial electrodes were digitized. As previously described [1], the electrode coordinates were projected onto a 2D polar plot, which is illustrated in Fig. 1. A triangular mesh was constructed to connect the neighboring electrodes in the polar projection. Using this triangular mesh, the signals were linearly interpolated from the electrodes onto a fine regular grid (100×100 grid points).

2. Signal analysis

As previously described [1], activation times were defined as the times at the minimum negative slope of the electrograms [12]. We assumed a minimum refractory period of 100 ms, and following an activation time, the subsequent activation for the same electrogram was assumed to occur between 100 ms and 300 ms later.

Electrical phase can be characterized using an angular representation given by the phase-plane plot of two state variables [13]. In order to compute phase, we first applied a signal detrending process similar to that used in [14]. This procedure consisted of subtracting from $V(\mathbf{x},t)$ a quadratic function between two successive activation times. The effect is that the voltage is zero at the minimum dV/dt (activation time), whilst the signal mean is also zero. The detrended signals obtained from this procedure are denoted $V_d(\mathbf{x},t)$ below. We computed the Hilbert transform [15] of the detrended signals $HV_d(\mathbf{x},t)$, and the phase $\varphi(\mathbf{x},t)$ was computed following [13] using

$$\varphi(\mathbf{x},t) = \text{atan2}(V_d(\mathbf{x},t), HV_d(\mathbf{x},t)). \tag{27}$$

Activation wavefronts are commonly idealized as one-dimensional lines separating tissue that has just been activated from tissue that is about to be activated. Wavefronts can be identified as the isochrones of the activation time. Due to the detrending step we have used, wavefronts can equivalently be identified using the isolines of zero detrended voltage (with negative dV/dt) or using the isolines of zero phase (under the Hilbert transform), which can be determined by tracking active edges [14]. Consequently, the use of the activation time (if it is well-defined everywhere), detrended voltage, or phase results in the same estimate of wavefront conduction velocity, due to the uniqueness of the conduction velocity regardless of the field used to define wavefronts.

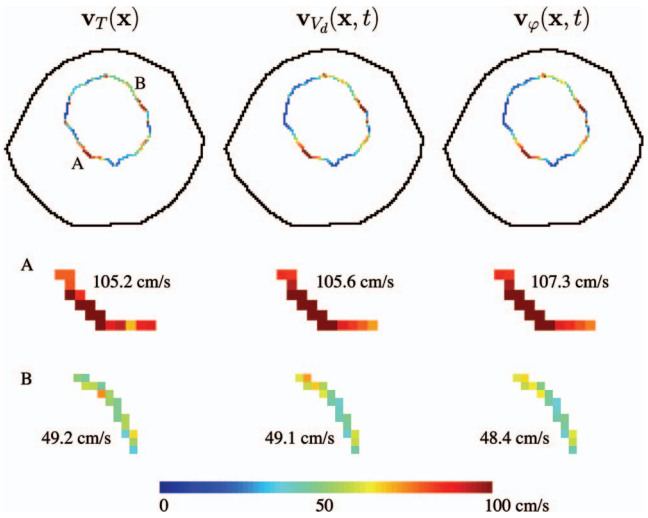

FIG. 2. (Color) An activation wavefront during a period of organized VF activity, showing conduction velocity estimates from activation time (left column), from detrended voltage (middle column), and from phase (right column) represented using a pseudocolor spectrum. Top panels illustrate the location of the activation wavefront using the 2D polar projection (see Fig. 1). For these maps, the mean conduction velocity magnitudes over all points on the wavefront were $|\mathbf{v}_T|=47.2$ cm/s, $|\mathbf{v}_{V_d}|=46.6$ cm/s, and $|\mathbf{v}_\varphi|=46.9$ cm/s. A local comparison of conduction velocity for the regions indicated by A and B are expanded in rows 2 and 3, respectively. For each panel, the value indicates the mean conduction velocity for the pixels shown.

We estimated the conduction velocity of the epicardial wavefronts using Eqs. (16) and (21). Consistent with previous similar studies, this corresponds to an *apparent* conduction velocity, since we do not have access to the electrical activity within the 3D volume (i.e., the measurements are restricted to the epicardial surface), thus we are unable to compute the true 3D conduction velocity.

B. Results

We determined the apparent conduction velocity on the ventricular epicardial surface of a fibrillating pig heart at several time instants. During a relatively organized period of VF activity, we compared conduction velocity estimates determined from the spatial fields of activation time, detrended voltage, and phase. We also quantified conduction velocities obtained from detrended voltage and phase during complex VF activity, for which the activation time field could not be determined.

1. Organized VF activity

We analyzed a short segment of organized activity, for which VF was driven by a single activation wavefront. Dur-

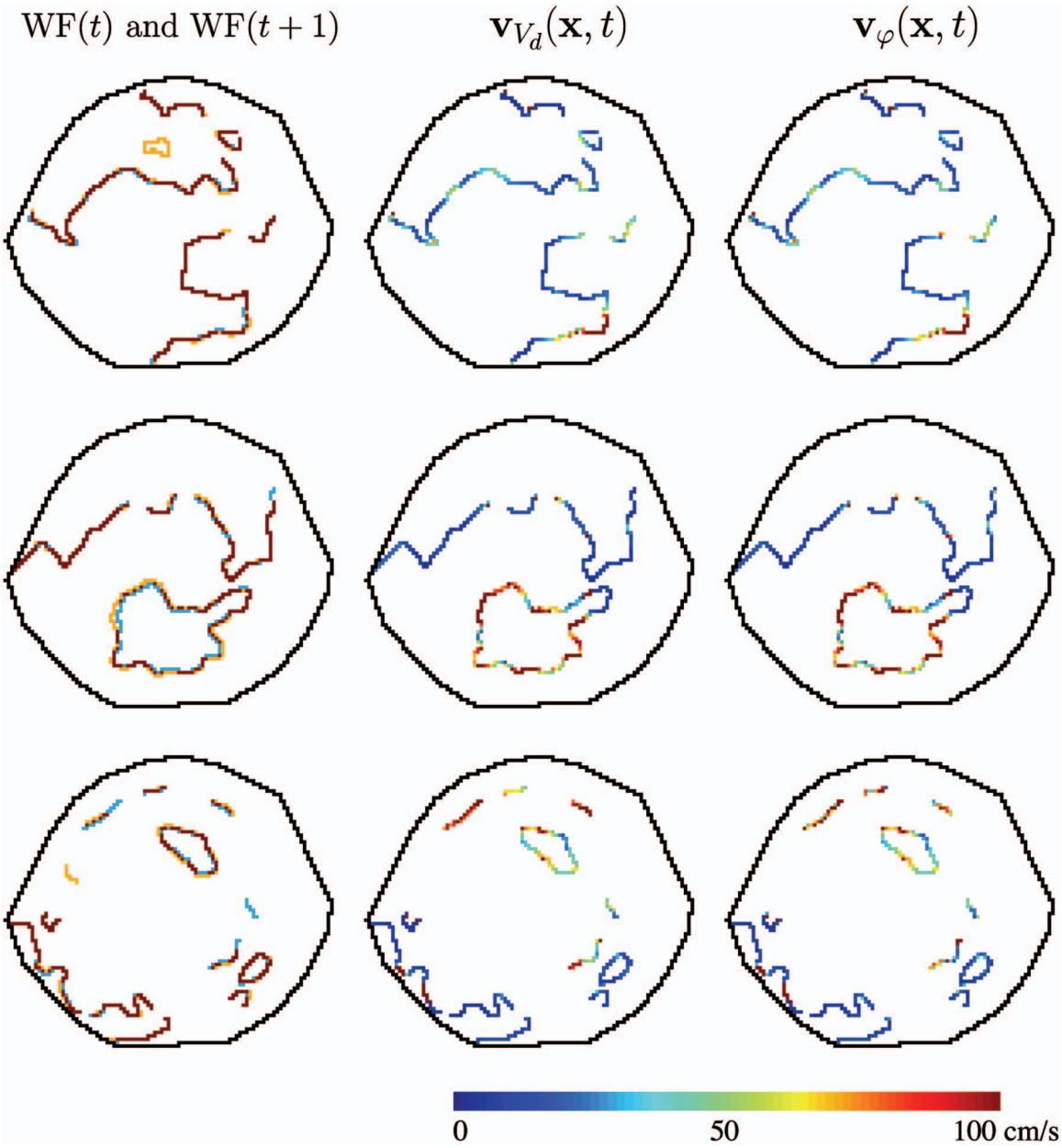

FIG. 3. (Color) Activation wavefronts at three time instants during complex VF. Left column: wavefronts at time t, WF(t) (light blue) plotted together with the wavefronts 1 ms later WF($t+1$) (orange). The pixels that belong to both wavefronts are represented in brown. Conduction velocity computed from detrended signals (middle column) and phase (right column) is indicated along the wavefronts using a pseudocolor spectrum. From top to bottom: across all wavefronts for each time instant, the mean conduction velocity magnitude $|\mathbf{v}_{V_d}|$ was 25.5 cm/s, 42.7 cm/s, and 30.4 cm/s, respectively, and the mean $|\mathbf{v}_{\varphi}|$ was 24.9 cm/s, 43.2 cm/s, and 31.9 cm/s, respectively.

ing this period, each point of the epicardium was activated just once, and could thus be assigned a unique activation time represented as $T(\mathbf{x})$ on the epicardial surface. Consequently, an appropriate choice for the required scalar field f was $f(\mathbf{x},t)=T(\mathbf{x})-t$, which enabled us to determine the conduction velocity over the entire epicardium using Eqs. (16) and (21). To compare with these estimates, we also computed conduction velocities using the detrended voltage or phase fields, for which we defined the function f in Eqs. (16) and (21) to be $V_d(\mathbf{x},t)$ or $\varphi(\mathbf{x},t)$, respectively.

Figure 2 illustrates a wavefront during the organized period of VF. The pseudocolor spectrum along the activation wavefront indicates the magnitude of the conduction velocity, which was computed using the scalar fields of activation time $\mathbf{v}_T$ (left), detrended voltage $\mathbf{v}_{V_d}$ (middle), and phase $\mathbf{v}_{\varphi}$ (right). We have shown that conduction velocities computed from these fields are theoretically equivalent. The data in Fig. 2 demonstrate the experimental equivalence of these estimates. Focusing on two portions of the wavefront (denoted A and B in Fig. 2) and using $\mathbf{v}_T$ as the reference, the local

estimates $\mathbf{v}_{V_d}$ and $\mathbf{v}_{\varphi}$ differed by 0.4% and 2%, respectively [portion A in Fig. 2], and 0.2% and 1.6%, respectively [portion B in Fig. 2]. The relative differences in the mean conduction velocity computed over the entire wavefront were 1.3% and 0.6%, respectively, compared to $\mathbf{v}_T$.

2. Complex VF activity

Figure 3 presents examples of activation wavefronts and their conduction velocities during complex VF activity. Illustrated in the left column are wavefronts at a particular time instant (light blue) together with the locations of the same wavefronts 1 ms later (orange). The pixels that belong to both wavefronts are colored brown (in which case, the wavefront motion between the time instants was very small). Similar conduction velocity estimates were determined from the spatial fields of detrended voltage (middle panels) and phase (right panels), although numerical issues led to minor differences in magnitude that were typically less than 2 cm/s. These epicardial conduction velocity estimates are consistent with previously published data from fibrillating pig hearts [7]. The portions of the wavefronts that moved substantially (as indicated in the left panels) were associated with the parts of the wavefront that had a high conduction velocity (red portions of the wavefronts in the middle and right panels). On the other hand, locations at which the wavefront was almost stationary had very low conduction velocity (blue) as expected.

IV. DISCUSSION

We have presented a general method for quantifying the conduction velocity of excitation wavefronts in the fibrillating heart. This method is based on tracking material particles that are assumed to be embedded within the propagating wavefronts, whilst the direction of the conduction velocity vector for each point on the wavefront is assumed to be perpendicular to the wavefront. We have followed several recent studies [3,5–7,9,10] in making this assumption, although this has attracted some controversy [16]. Our method relies on using a given direction of conduction and solving a particle derivative expression [Eq. (9)] in order to obtain the conduction velocity magnitude. Hence, it would be straightforward to incorporate a different conduction direction.

Previously published methods to estimate conduction velocity have typically relied on computing gradients of the activation time field, and this has been successfully applied to characterize organized electrical activity [6,7]. Our overall aim was to study complex VF activity, for which the computation of an activation time field (and hence its gradient) is ambiguous [7,17], since some sites may be activated twice or more over a specific period, whilst others may not be activated at all during this period. In the absence of spatiotemporal gradients of the activation time field, the conduction velocity cannot be determined using conventional methods. On the other hand, phase analysis is a well-established technique for studying the complex electrical activity during VF [14]. Activation wavefronts correspond to the isolines of zero detrended voltage (with negative dV/dt), and thus to the isolines of zero phase under the Hilbert transform. Moreover, detrended voltage and phase, and their spatial gradients, are well defined everywhere at all times.

In this paper, we have shown that the conduction velocity can equivalently be calculated from the spatial fields of activation time, phase, or indeed any other scalar field for which a particular isovalue defines the activation wavefronts. We derived an explicit expression for the conduction velocity in terms of the spatiotemporal gradients of the scalar field used to define wavefronts [Eq. (12)]. We demonstrated that existing methods for estimating conduction velocity from activation times in 2D [7] and 3D [6] are specific cases of this general method. We have also shown how our formulation can be transformed to determine conduction velocity from epicardial surface recordings using Eqs. (16) and (21).

To complement our theoretical findings, we analyzed a period of organized electrical activity recorded from the epicardium of the pig heart, and demonstrated the equivalence of conduction velocity estimates as determined from the experimentally derived activation times, phase, and detrended voltage. We observed minor differences in these numerical estimates that are likely to be due to the finite difference approximations of the spatial and temporal derivatives of the various fields. We also observed small differences in the conduction velocity estimates computed from phase and from detrended voltage during complex VF activity in the pig heart. This suggests that our method is an improvement over previous methods, because our analysis of complex VF does not require the calculation of an activation time field.

We have developed and illustrated the applicability of a method for estimating conduction velocity during complex multiple-wavelet VF. Quantification of conduction velocity and its dynamic restitution properties in the intact fibrillating heart will help to provide insight into the mechanisms underlying VF, which may in turn inform the design of therapies to prevent or terminate VF.

ACKNOWLEDGMENTS

The experimental data was recorded in collaboration with Prof. David Paterson and Dr Chris Bradley. We are also grateful for the valuable discussions with Drs. Peter Taggart and Richard Clayton.

APPENDIX: DERIVATION OF A WAVEFRONT TANGENT VECTOR

At any time t, a wavefront on the surface $\mathbf{S}(u,v)$ given by Eq. (14) can be parametrized using $\mathbf{S}(u(s),v(s))$, where s is an arc length parameter that varies along the wavefront. A vector $\boldsymbol{\tau}$ that is tangent to the wavefront can be obtained by differentiating $\mathbf{S}(u(s),v(s))$ with respect to s as follows:

$$\boldsymbol{\tau} = \frac{\partial \mathbf{S}}{\partial u}\frac{du}{ds} + \frac{\partial \mathbf{S}}{\partial v}\frac{dv}{ds}. \tag{A1}$$

On the other hand, the wavefront is defined as the zero isoline of f, which implies that $f(u(s),v(s),t)=0$. Differentiating this with respect to s gives

$$\frac{\partial f}{\partial u}\frac{du}{ds} + \frac{\partial f}{\partial v}\frac{dv}{ds} = 0. \tag{A2}$$

Solving this equation, we obtain

$$\frac{du}{ds} = c\frac{\partial f}{\partial v}, \quad \frac{dv}{ds} = -c\frac{\partial f}{\partial u}. \tag{A3}$$

Combining Eq. (A1) and Eq. (A3) we obtain an expression for the wavefront tangent vector:

$$\boldsymbol{\tau} = \frac{\partial \mathbf{S}}{\partial u}\frac{\partial f}{\partial v} - \frac{\partial \mathbf{S}}{\partial v}\frac{\partial f}{\partial u}. \tag{A4}$$

[1] M. P. Nash, A. Mourad, R. H. Clayton, P. M. Sutton, C. P. Bradley, M. Hayward, D. J. Paterson, and P. Taggart, Circulation **114**, 536 (2006).

[2] R. Wolk, S. M. Cobbe, M. N. Hicks, and K. A. Kane, Pharmacol. Ther. **84**, 207 (1999).

[3] R. A. Gray, A. M. Pertsov, and J. Jalife, Circulation **94**, 2649 (1996).

[4] Y. Y. Kwan, W. Fan, D. Hough, J. J. Lee, M. C. Fishbein, H. S. Karagueuzian, and P.-S. Chen, Circulation **97**, 1828 (1998).

[5] F. J. Chorro, J. Cánoves, J. Guerrero, L. Mainar, J. Sanchis, L. Such, and V. Lopez-Merino, Circulation **101**, 1606 (2000).

[6] A. R. Barnette, P. V. Bayly, S. Zhang, G. P. Walcott, R. E. Ideker, and W. M. Smith, IEEE Trans. Biomed. Eng. **47**, 1027 (2000).

[7] P. V. Bayly, B. H. KenKnight, J. M. Rogers, R. E. Hillsley, R. E. Ideker, and W. M. Smith, IEEE Trans. Biomed. Eng. **45**, 563 (1998).

[8] D. Sung, J. H. Omens, and A. D. McCulloch, Ann. Biomed. Eng. **28**, 1085 (2000).

[9] M. W. Kay and R. A. Gray, IEEE Trans. Biomed. Eng. **52**, 50 (2005).

[10] M. J. Reiter, M. Landers, Z. Zetelaki, C. J. H. Kirchhof, and M. A. Allessie, Circulation **96**, 4050 (1997).

[11] M. P. Nash, C. P. Bradley, and D. J. Paterson, Circulation **107**, 2257 (2003).

[12] C. Haws and R. Lux, Circulation **81**, 281 (1990).

[13] R. A. Gray, A. M. Pertsov, and J. Jalife, Nature (London) **392**, 75 (1998).

[14] J. M. Rogers, IEEE Trans. Biomed. Eng. **51**, 56 (2004).

[15] M. A. Bray and J. P. Wikswo, Phys. Rev. E **65**, 051902 (2002).

[16] A. T. Winfree, IEEE Trans. Biomed. Eng. **43**, 1200 (1996).

[17] J. M. Rogers, M. Usui, B. H. KenKnight, R. E. Ideker, and W. M. Smith, Ann. Biomed. Eng. **25**, 749 (1997).